In-plane magnetic field studies of InAs/GaSb superlattices

A. R. Rundell, G. P. Srivastava, and J. C. Inkson
Department of Physics, University of Exeter, Stocker Road, Exeter EX4 4QL, United Kingdom
(Received 17 July 1996)

We present a theoretical study of electron and hole states in InAs/GaSb superlattices using a realistic microscopic pseudopotential complex-band-structure approach. A rectangular potential is used to predict the critical in-plane magnetic field that will result in a semiconducting state for a variety of InAs/GaSb superlattices. It is found that the critical field is insensitive to increases in superlattice period beyond a particular value. [S0163-1829(97)00508-0]

I. INTRODUCTION

InAs/GaSb semiconductor heterostructures have the unusual property that the InAs conduction band lies ~150 meV below the valence-band edge of the GaSb material.[1] Fermi-energy equalization throughout the structure then leads to the spontaneous creation of spatially separate hole- and electron-accumulation layers at the interface. Within InAs/GaSb superlattices, quantum confinement serves to raise (lower) the energy of the electron (hole) states — the size of the confinement energy increasing with decreasing layer width. Thus, for a superlattice with a narrow period there is no effective band overlap resulting in a semiconducting state. In a superlattice constructed from InAs(100 Å)/GaSb(30 Å), the sum of the confinement energies of the electron and hole subbands approximate to the band overlap. Larger periods will result in a semimetallic phase (i.e., both holes and electrons present).

All semimetallic InAs/GaSb heterostructures can undergo the transition to a semiconducting state by the application of a magnetic field or by the application of pressure. The magnetic field induced transition may be understood by considering a superlattice period such that there are two occupied electron levels (E_0 and E_1) in the InAs material and one hole level (H_0) in the GaSb material. As shown in Fig. 1(a), the Fermi level lies above the occupied electron subbands and below the occupied hole subband and hence the system is semimetallic at zero field. The application of a magnetic field will increase the energy of the electron states and lower the energy of the hole states due to the increased confinement. At some critical value of magnetic field, the highest-hole level will lie at a lower energy than the lowest-electron level [see Fig. 1(b)], resulting in complete carrier transfer back across the interfaces. At higher magnetic fields there will be the formation of an energy gap — the system is then semiconducting. This process is independent of the direction of the applied magnetic field, though the strength of the field required to affect the transition will be quite different for different geometries. For the case of a perpendicular magnetic field, quasi-zero-dimensional (0D) states are formed as magnetic confinement and superlattice confinement act in different directions. Thus, relatively low magnetic fields are required to affect the transition. In the parallel geometry, quasi-one-dimensional (1D) states are formed. In this case, magnetic field localization reduces the effect of superlattice confinement for states an orbit radius from an interface. This leads in the limiting case of a heterojunction, and also a long period superlattice, to the transition occurring between bulk-like Landau levels. Thus, higher magnetic fields are required to induce the semimetal-to-semiconductor transition. Clearly, this transition to semiconducting behavior will have dramatic effects on the transport properties of the system.

Considerable work[2–9] has been carried out on the semimetal-to-semiconductor transition in InAs/GaSb superlattices with the field applied perpendicular to the interfaces (i.e., parallel to the growth direction). For a typical superlattice (103 Å InAs/158 Å GaSb), Barnes *et al.*[4] have shown that the semimetal-to-semiconductor transition occurs between 40 T and 50 T. In the perpendicular geometry, the size of the field required to cause the transition is proportional to the energy difference between the lowest occupied electron state and highest occupied hole state at zero field. An increase in the InAs (or GaSb) layer width will result in an increase in the effective band overlap, and hence increase in the size of the critical magnetic field. Correspondingly a decrease in the layer width will lead to a reduction in the magnitude of the critical magnetic field.[4] This is because the confinement energies of the subbands at zero field will be greater, thus reducing the energy difference between the highest hole states and lowest electron states.

Experimental work has also been performed on InAs/GaSb quantum wells,[7] which clearly demonstrate the semimetal-to-semiconductor transition upon the application of magnetic field. Theoretical studies of these systems have been conducted using the $\mathbf{k}\cdot\mathbf{p}$ method.[2–4,8] A 200 Å InAs/50 Å GaSb superlattice has been shown to have a critical field of 36 T.[4] In this system the electron and hole states become

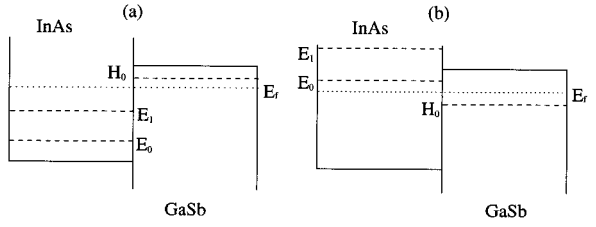

FIG. 1. The magnetic field induced semimetal-to-semiconductor transition for an InAs/GaSb superlattice (a) $B<B_{\text{critical}}$ (b) $B>B_{\text{critical}}$.

coincident in energy and mix strongly; thus it is critical that a comprehensive treatment of the states is considered for an accurate representation of the dispersion (and hence uncrossing) of the Landau levels with magnetic field.

To our knowledge there is no published work that examines the semimetal-to-semiconductor transition in InAs/GaSb superlattices subjected to an in-plane magnetic field. In this work we examine this problem using a realistic microscopic pseudopotential approach. This method is ideal for the study of InAs/GaSb superlattices with a magnetic field applied parallel to the interfaces. Hamiltonian periodicity is destroyed due to the magnetic field and hence a finite superlattice must be studied for an accurate representation of the physical system. The predicted critical in-plane field required to induce the semimetal-to-semiconductor transition is found to depend upon the energy difference between the lowest-electron and highest-hole subbands at zero field. Section II contains a description of the theoretical method used, and in Sec. III we shall present the results and give a discussion.

II. THEORY

In order to determine the single-particle states in InAs/GaSb heterostructures, we use a complex-band-structure method,[10–14] based on local empirical pseudopotentials[15] and a layer boundary condition.[13,14]

If z represents the growth direction, the Schrödinger equation for the system can be written as

$$\left[-\frac{\hbar^2\nabla^2}{2m}+V(\mathbf{r})\right]\Psi(\mathbf{r})=E\Psi(\mathbf{r}), \tag{1}$$

where the crystal potential V is given as

$$V=\begin{cases} V_{\mathrm{InAs}}, & z\in \text{InAs region} \\ \Delta+V_{\mathrm{GaSb}}, & z\in \text{GaSb region,} \end{cases} \tag{2}$$

with Δ as the appropriate band offset between InAs and GaSb, which gives the band overlap between the conduction band edge of InAs and valence band edge of GaSb as 150 meV. We use a plane wave expansion for the wave function:

$$\psi_{\mathbf{k}}(\mathbf{r})=\sum_{\mathbf{G}} A_{\mathbf{k}}(\mathbf{G})e^{i(\mathbf{k}+\mathbf{G})\cdot\mathbf{r}}. \tag{3}$$

and a similar Fourier expansion for the microscopic crystal potential. Then Eq. (1) can be expressed as[16]

$$\sum_{\mathbf{G}} H_{\mathbf{G}'\mathbf{G}}(\mathbf{k})A_{\mathbf{k}}(\mathbf{G})=0, \tag{4}$$

where

$$H_{\mathbf{G}'\mathbf{G}}(\mathbf{k})=\left[\left\{\frac{\hbar^2}{2m}(\mathbf{k}+\mathbf{G})^2-E\right\}\delta_{\mathbf{G}',\mathbf{G}}+V^{\mathrm{ps}}(\mathbf{G}'-\mathbf{G})\right]. \tag{5}$$

Here $V^{\mathrm{ps}}(\mathbf{G}-\mathbf{G}')=v(|\mathbf{G}-\mathbf{G}'|)S(\mathbf{G}-\mathbf{G}')$ is the microscopic crystal pseudopotential and is written as a product of the structure factor and the pseudopotential form factors.[17]

It is important to include the effects of spin-orbit coupling in the present study. The spin-orbit interaction in real space is

$$H_{\mathrm{so}}=\frac{\hbar^2}{4m^2c^2}(\nabla V\times\mathbf{p})\cdot\boldsymbol{\sigma}. \tag{6}$$

In momentum space, the spin-orbit matrix element is given by[18]

$$H^{\mathrm{so}}_{\mathbf{G}'\mathbf{G}}=-i\Lambda(\mathbf{G}-\mathbf{G}')\boldsymbol{\sigma}\cdot[(\mathbf{k}+\mathbf{G})\times(\mathbf{k}+\mathbf{G}')], \tag{7}$$

where $\Lambda(\mathbf{G}-\mathbf{G}')=\lambda S(\mathbf{G}-\mathbf{G}')$ is the strength of the spin-orbit interaction. With the inclusion of the spin-orbit interaction, each element of $\mathrm{H}_{\mathbf{GG}'}$ becomes a 2×2 matrix, and the wave function is a spinor.

In a real semiconductor heterostructure, crystal symmetry is retained in two directions, but in the third (the growth direction) the symmetry is broken. For a given incident parallel momentum and energy one must solve Eq. (5) for allowed values of k_z. This equation can be made linear by forming a polynomial expansion in k_z,[12]

$$H_{\mathbf{GG}'}(\mathbf{k})=H_2k_z^2+H_1k_z+H_0, \tag{8}$$

with

$$H_2=\frac{\hbar^2}{2m}\delta_{\mathbf{GG}'},$$

$$H_1=\frac{\hbar^2}{m}g_z\delta_{\mathbf{GG}'}, \tag{9}$$

$$H_0=\left[\frac{\hbar^2}{2m}(\mathbf{k}_\parallel{}^2+\mathbf{g}_\parallel{}^2+g_z^2)-E\right]\delta_{\mathbf{GG}'}+V(\mathbf{G}-\mathbf{G}').$$

This process must also be performed on the spin-orbit part of the equation, giving

$$H^{\mathrm{so}}=(H^{\uparrow\downarrow}_{\mathrm{so}_1}+H^{\downarrow\uparrow}_{\mathrm{so}_1})k_z+(H^{\uparrow\uparrow}_{\mathrm{so}}+H^{\uparrow\downarrow}_{\mathrm{so}}+H^{\downarrow\uparrow}_{\mathrm{so}}+H^{\downarrow\downarrow}_{\mathrm{so}}), \tag{10}$$

with

$$H^{\uparrow\downarrow}_{\mathrm{so}_1}=\Lambda[G_x+iG_y],$$

$$H^{\downarrow\uparrow}_{\mathrm{so}_1}=\Lambda[-G_x+iG_y],$$

$$H^{\uparrow\uparrow}_{\mathrm{so}}=i\Lambda[G_x(k_y+G_y)-G_y(k_x+G_x)],$$

$$H^{\uparrow\downarrow}_{\mathrm{so}}=\Lambda\{-G_z[k_x+G_x+i(k_y+G_y)]+G_xG_z+iG_yG_z\}, \tag{11}$$

$$H^{\downarrow\uparrow}_{\mathrm{so}}=-\Lambda\{-G_z[k_x+G_x-i(k_y+G_y)]+G_xG_z-iG_yG_z\},$$

$$H^{\downarrow\downarrow}_{\mathrm{so}}=-i\Lambda[G_x(k_y+G_y)-G_y(k_x+G_x)].$$

Hence the matrix in Eq. (5) may now be written as

$$\begin{bmatrix} 0 & 0 & 1 & 0 \\ 0 & 0 & 0 & 1 \\ H_2^{-1}(H_0 - H_{so}^{\uparrow\uparrow}) & -H_{so}^{\uparrow\downarrow} & H_2^{-1}H_1 & -H_{so_1}^{\uparrow\downarrow} \\ (H_{so}^{\uparrow\downarrow})^* & H_2^{-1}(H_0 + H_{so}^{\uparrow\uparrow}) & (H_{so_1}^{\uparrow\downarrow})^* & H_2^{-1}H_1 \end{bmatrix} \begin{bmatrix} A\uparrow \\ A\downarrow \\ k_z A\uparrow \\ k_z A\downarrow \end{bmatrix} = k_z \begin{bmatrix} A\uparrow \\ A\downarrow \\ k_z A\uparrow \\ k_z A\downarrow \end{bmatrix}. \quad (12)$$

The eigenvalues of this matrix equation are the allowed values of the perpendicular component of the electron wave vector. The eigenfunctions are the coefficients of the wavefunction expansion and the derivatives of the wavefunction with respect to k_z. Hence, given an incident parallel component of wave vector and an energy range, the complex band structure for a given material may be computed easily.

For a superlattice calculation we consider a finite number of InAs/GaSb layers along the growth direction. Once the layer-wave-function coefficients are determined, the transmission coefficient and wave function in the heterostructure are found using a scattering matrix approach as described in earlier publications.[13,14,19] Bound states within a structure can be identified by searching for energies at which coefficients in the scattering matrix become very large and then calculating the wave function at these energies. The method is highly flexible since it does not require that the heterostructure under consideration be periodic in the growth direction.

Application of an in-plane magnetic field to the structure is considered by digitizing the vector potential: the structure is divided into a number of artificial layers and the vector potential is taken as a constant in each layer as shown in Fig. 2.[14] The effect of the digitization procedure is to change the parallel momentum such that in the ith layer;[14]

$$\mathbf{k}_{||i} \rightarrow \mathbf{k}_{||} + \frac{e\mathbf{A}_i}{\hbar}, \quad (13)$$

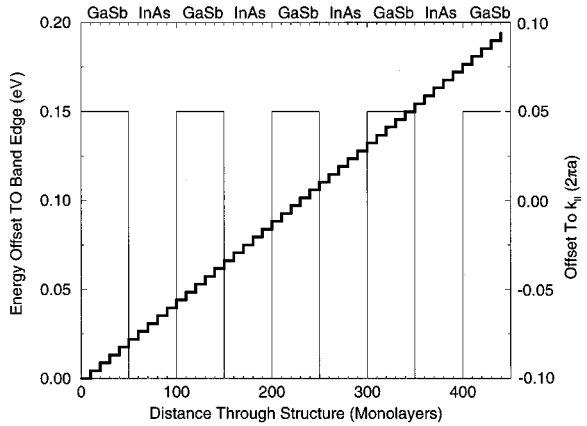

FIG. 2. The InAs/GaSb superlattice structure under consideration (left scale) and the digitization of the magnetic vector potential (thick line) (right scale). The digitization length is taken as 10 monolayers, indicated by the small tickmarks on the diagram, thus each material contains five artificial layers. The cyclotron center is at the edge of the structure.

where $\mathbf{A}_i$ is the vector potential in the layer. The procedure will not adversely affect the results produced by the method if the digitization (artificial layer) width is smaller than the magnetic length.[18] Having fully specified the Hamiltonian Eq. (12) can now be solved.

The center of the electron Landau orbit (cyclotron center) lies within the layer where the in-plane wave vector $k_{||,i}$ is zero, e.g., the central layer in Fig. 2. Hence, the cyclotron-center-dependent dispersion of the states can be examined by changing the initial value of the parallel wave vector, as this will result in a change of the layer where the in-plane wave vector is zero.

The digitization of the vector potential is compatible with the inclusion of electrostatic potentials. For example, for an InAs/GaSb heterojunction, a Thomas-Fermi approximation may be used to simulate the band bending at the interface.[25] In that case a functional form for the electrostatic potential is taken and digitized in the above fashion. The change in the value of the potential at an artificial interface is then included as an offset to the energy in Eq. (9), i.e., it changes the energy position of the band edge.

III. RESULTS AND DISCUSSION FOR THE InAs/GaSb SUPERLATTICE

A. Superlattice in zero magnetic field

The interface potential was assumed to be of a rectangular form for all superlattices under consideration, with the band overlap set to 150 meV as indicated in Fig. 2. Under increasing magnetic field, charge recombines across the interface as corresponding Landau levels pass through the Fermi energy. Hence, at the critical transition field (the field that results in the recombination of the last free charge) no charge is present to screen the band offset and thus a rectangular potential is accurate at the transition field. If the InAs or GaSb layer width is less than ~100 monolayers there is negligible band bending and so the rectangular potential also represents a good approximation at zero field.[20]

A InAs(211 Å)/GaSb(30 Å) superlattice is first examined for the case of no applied magnetic field. In order to minimize computational time, the smallest structure which not does compromise the results is required. Here we consider the transmission through a four-, five-, and six-period superlattice.

Figure 3 shows the transmission spectra corresponding to the four-, five-, and six-period superlattices. There are three wide plateaus which begin at ~ 20 meV, 75 meV, and 150 meV above the bulk InAs conduction band bottom, which correspond to the ground-, first-excited and second-excited electron (InAs) minibands, respectively. The widths of the minibands increase for the higher excited states, which is a

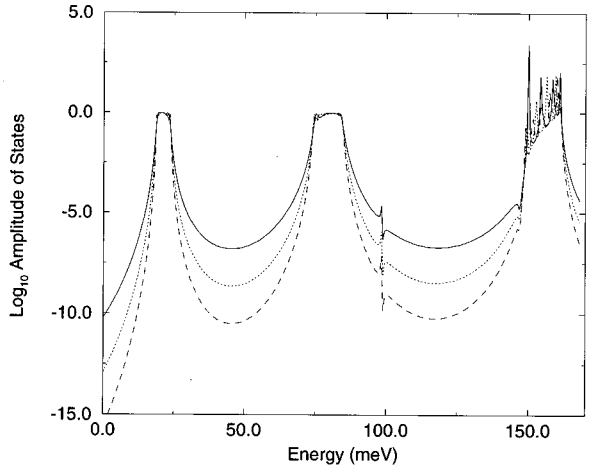

FIG. 3. The transmission coefficient for an electron incident on a four- (solid line), five- (dotted line), and six- (dashed line) period InAs/GaSb superlattice. The energy reference is at the bottom of the bulk InAs conduction band.

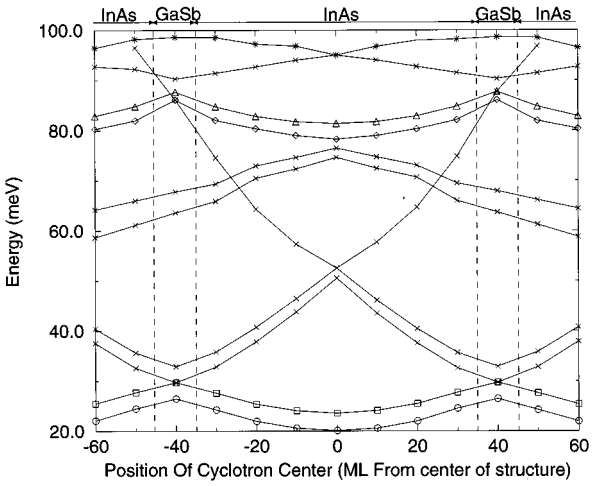

FIG. 4. The cyclotron dispersion of the major states in an 211 Å InAs, 30 Å GaSb superlattice at 5 T. The energy reference is at the bottom of the InAs conduction band. ○ represents a spin-up lowest-electron state, □ a spin-down lowest-electron state, ◇ a spin-up first excited electron state, △ a spin-down first excited electron state, * the highest-hole state, and × the antisymmetric combinations of the highlighted states.

consequence of increased wave-function overlap between the quantum well states. The increased overlap can be more readily seen for the second-excited miniband, which contains a finite number of peaks highlighting the nonperiodic (i.e., finite) nature of the structure. The number of peaks in the miniband corresponds to the number of wells in the structure and the miniband widths do not increase significantly with increasing periods.[21] The narrow resonance-antiresonance feature 100 meV above the bulk InAs conduction band bottom corresponds to the highest-hole (GaSb) state. There is little interaction between the states in successive GaSb layers due to the large InAs layer width. All the superlattices shown are semimetallic since the highest-hole state lies $\sim$80 meV above the low energy edge of the electron ground miniband.

The difference between the spectra for the superlattices is not significant. Moreover, the position of the lowest electron state at 10 T varies by less than 0.1 meV between the structures. This is much smaller than the cyclotron energy of electrons in the InAs material (5 meV T^{-1}) and thus an increase in the number of periods will not significantly improve the accuracy of the predicted transition fields. The behavior of a four-period superlattice is thus a good approximation to that of a superlattice with a much larger number of periods, as has been shown experimentally[23] and theoretically.[21]

At zero field the subband density of states can be approximated to that of a two-dimensional electron gas. Since the miniband width is narrow this is a very good approximation for the holes, as the GaSb layers are behaving as isolated quantum wells, and is also reasonable for the electron states.[22] Taking the experimental band-edge values of for the effective mass of the electrons ($0.023m_e$) in InAs, and heavy holes ($0.33m_e$) in GaSb the Fermi energy lies 73 meV above the lowest-electron subband. From Fig. 3 this indicates that the first two electron subbands and the highest-hole subband are occupied.

B. Superlattice in finite magnetic field

An in-plane magnetic field will split the electron and hole subbands into quasi-one-dimensional (1D) Landau levels. This increased confinement will force the electron levels to a higher energy and the hole levels to a lower energy. Using the Landau gauge for the vector potential, the dispersion of the Landau levels with k_x remains free particlelike, and a dispersion of the form $\hbar^2 k_x^2/2m^*_{e,h}$ is expected with a minimum in the energy of the Landau level at $k_x=0$. The dispersion of the Landau levels in the k_y direction is critical because a change in k_y will alter the cyclotron center. Figure 4 shows the dispersion of several of the lowest-electron and the highest-hole states with a cyclotron center for an in-plane magnetic field of 5 T. This dispersion is typical of electron and hole states in superlattices under in-plane magnetic fields.[14]

The form of the electron dispersion in Fig. 4 is due to the interaction (i.e., anticrossing) between the electron states within the GaSb layers and the hole states within the InAs layers, as well as interaction between neighboring electron and hole states; these interactions lead to the appearance of definite bands. The interaction between the lowest-electron states is depicted in Fig. 5. It is clear that there is considerable interaction between the states of like spin. The two spin-up electron states from each side of the GaSb layer anticross leading to two distinct bands *AC* (reading left to right) at the lower energy and *CA* at the higher energy. The minimum gap between the different combinations is $\sim$3 meV at the center of the GaSb layer. The situation is the same for the spin-down states, but as is clear from Fig. 5, opposite spin states do not interact. The upper (antisymmetric) electron state has the minimum of its dispersion in the GaSb material, where it interacts with the symmetric electron state. The strength of this interaction is weaker because the electron states are now separated by more than 10 monolayers of GaSb — this reduces the anticrossing gap to $\sim$1.9 meV. This higher electron state does not interact significantly with any of the other states shown due to the large spatial separation between states in that band.

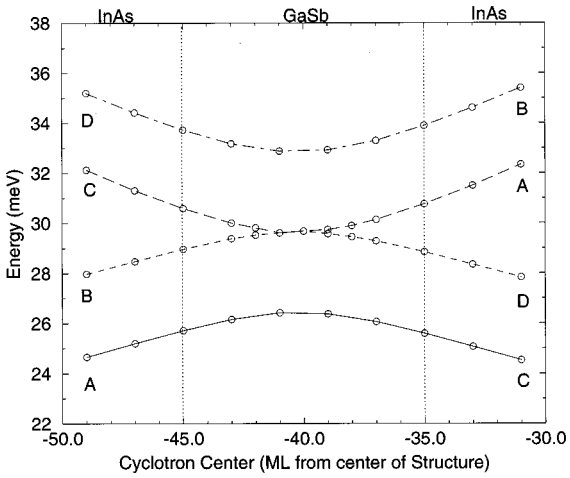

FIG. 5. The anticrossing of electron levels around a GaSb layer. The lowest spin-up electron states anticross forming the *AC* (solid line) and *CA* (dashed line) bands. The lowest spin-down electron states anticross to form the *BD* (dotted line) and *DB* (dot-dashed line) bands. There is no interaction between states of different spin.

A similar description applies for the hole levels. Figure 6 shows the hole levels anticrossing in the center of an InAs layer. The interaction between the hole states is clearly weaker and the size of the gap between the hole states is $\sim$1.3 meV. This is a consequence of the greater separation between the hole levels, which serves to reduce the wave function overlap and thus the magnitude of the interaction.

There is a more pronounced dispersion of the electron and hole states with a cyclotron center as the magnetic field becomes stronger. This is due to the fact that when the magnetic length is of the order of the superlattice period, the Landau energy reflects directly the superlattice potential. Figure 7 shows the cyclotron-center dispersion of the spin-up and spin-down components of the lowest-electron state, and the highest-hole state under an in-plane magnetic field of 55 T. The flat region exhibited by the electron states occurs when the Landau orbit is confined to the InAs and

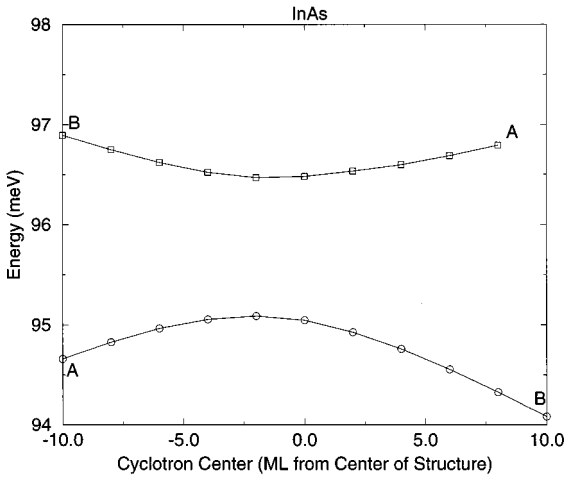

FIG. 6. The highest-hole states from neighboring GaSb quantum wells anticrossing in the center of an InAs layer forming the *BA* band (□) and the *AB* band (○).

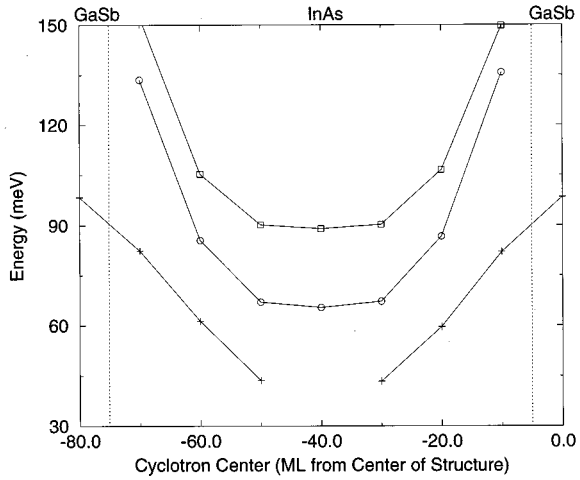

FIG. 7. The cyclotron dispersion of the lowest-electron level, and the highest-hole level in the 211 Å InAs, 30 Å GaSb superlattice at 55 T. The energy zero is taken at the top of the bulk InAs conduction band. ○ represents the spin-up lowest-electron state, □ the spin-down lowest-electron state, and + the highest-hole state.

hence the states lying in this region are effectively ''bulk'' Landau levels. The width of this region depends upon the relative sizes of the magnetic length and the superlattice layer width. Bulk Landau levels will exist in the center of the layer, and persist until the cyclotron center is shifted to within a cyclotron orbit radius of a material interface. There are no bulk GaSb Landau levels at this magnetic field since the magnetic length is longer than the GaSb layer width. Thus, to estimate the transition field, the dispersion of the electron and hole states with k_y must be examined, with k_x set to zero.

C. The semimetal-to-semiconductor transition

The heterostructure will be semiconducting when no GaSb valence-band states lie higher in energy than InAs conduction-band states. When both layer widths in the superlattice are very long, the transition will occur for bulklike states when $\frac{1}{2}\hbar\omega_c^{\mathrm{elec}}+\frac{1}{2}\hbar\omega_c^{\mathrm{hole}}$ is equal to the band overlap (150 meV). Taking the bulk values of the band-edge effective masses ($0.023m_e$ for electrons[24] and $0.33m_e$ for holes[24]) this gives a critical field strength of $\sim$56 T. The value of the critical field required to turn the system semiconducting is a function of the InAs and GaSb width. For a fixed GaSb width, the transition field will increase with increasing InAs layer thickness up to a critical InAs layer width, after which the transition field will remain constant as a result of the appearance of the bulk states in the InAs layers. For the in-plane magnetic field the critical InAs width is found to be $\sim$120 Å. Figure 8 shows how the energy difference between the lowest-electron state and the highest-hole state changes as a function of magnetic field for a variety of superlattices.

For the InAs(210 Å)/GaSb(30 Å) superlattice the magnitude of the energy difference decreases with increasing magnetic field until, at $\sim$58 T, the system becomes semiconducting. There is no effective increase in confinement (i.e., energy) until the magnetic length is shorter than the material

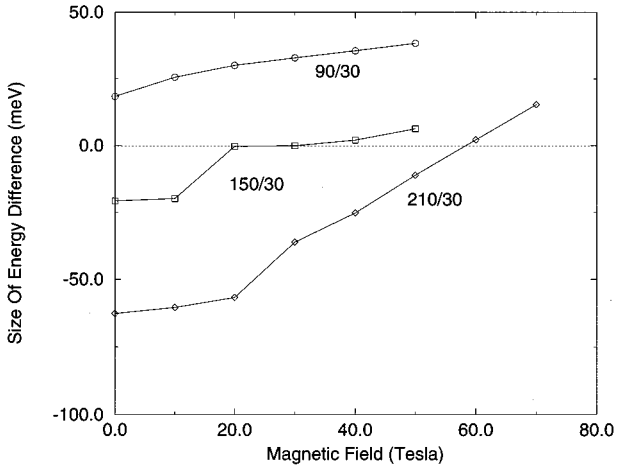

FIG. 8. Variation in the energy difference between the lowest-electron state and highest-hole state with increasing magnetic field for several different InAs layer widths. All the structures have a GaSb width of 30 Å and InAs widths of ○—90 Å; □—150 Å; ◇—210 Å.

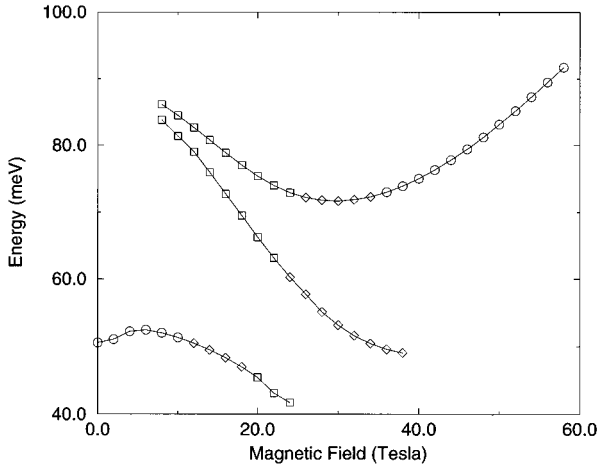

FIG. 9. Anticrossing features of the lowest-electron state and highest-hole states within an InAs layer. ○ are states with electronlike character, □ are states with holelike character, and ◇ are states with mixed character.

width in the superlattice. For the InAs layers considered here this occurs at ~20 T. Thereafter the electron states in the center of the InAs layers do not experience the superlattice confinement, and the semimetal-to-semiconductor transition occurs when the bulk like InAs Landau levels pass to a higher energy than the hole states in the GaSb material. In the high field regime the reduction in energy difference is approximately linear with field, and the effective mass which is calculated from this dependence is twice the band-edge effective mass in InAs. This enhancement is due to the nonparabolic effects in InAs and the interaction with the hole levels in the superlattice. The hole states do not develop into bulk Landau levels for the fields shown due to the much narrower GaSb width in this superlattice, although the hole states begin to feel the influence of the magnetic confinement at ~55 T — just as the system becomes semiconducting.

The behavior of InAs(90 Å)/GaSb(30 Å) superlattice is straightforward. The sum of superlattice confinement energies of the electron and hole subbands is greater than the band overlap, resulting in a semiconducting state at zero field. Subsequent increases in magnetic field force the electron and hole states further apart thus increasing the energy difference. This increase is not linear due to nonparabolic effects, particularly in the InAs material.

The situation is more complex in superlattices with intermediate InAs widths. For example, in the InAs(150 Å)/GaSb(30 Å) superlattice the magnetic length is comparable to the width of the InAs layer as the lowest-electron state passes the highest-hole state. As a result, there is considerable interaction between the two states keeping the system semimetallic over a larger range of magnetic field.

Figure 9 shows the effect of interaction between hole states (arising from GaSb corresponding to orbits centered in the InAs layer) and the highest available electron state. The highest-hole state changes character from holelike at low magnetic fields to electronlike at high field, while the reverse is true for the lowest state. The middle state remains essentially holelike but switches nodal character reflecting the energy order at high magnetic fields. The minimum size of the gap between the lowest electron and highest hole state is of the order of 30 meV and is the result of a substantial wave-function overlap. There is an initial rise in the energy of the lowest electron state before it gains considerable holelike character, and moves to a lower energy as the magnetic field is increased from ~ 7 T to ~ 22 T. The energy difference between the highest-hole state in this system and the lowest-electron state increases from 40 meV to nearly 50 meV over this field range, i.e., the system becomes more metallic as the magnetic field increases. However, beyond 40 T the upper state becomes electronlike and exhibits a bulklike dispersion and the system becomes semiconducting at ~58 T.

Similar behavior is seen in the InAs(120 Å)/GaSb(30 Å) superlattice, although the magnetic length now becomes shorter than the InAs layer width at ~30 T, which coincides with the transition to a semiconducting state. The situation is similar as the InAs width increases, albeit to a lesser extent. The InAs(180 Å)/GaSb(30 Å) superlattice has an anticrossing gap of 17 meV and no significant increase in the effective energy difference. In InAs(210 Å)/GaSb(30 Å) superlattice this anticrossing gap has reduced to 3 meV.

Increasing the GaSb width will serve to increase the critical transition field, since a wider GaSb period will result in a reduction in the confinement energy for the hole states, thus generating a larger band overlap at zero field. As an example, we calculate that a InAs(120 Å)/GaSb(120 Å) superlattice undergoes the semimetal-to-semiconductor transition at ~90 T. In this case there is little interaction between the lowest-electron and highest-hole states close to the transition field, because the magnetic length is shorter than 120 Å resulting in a suppression of the wave function overlap. The lowest energy electron state will be the bulk Landau level in InAs, and similarly the highest energy hole state will be the bulk Landau level in GaSb. Once these Landau levels are produced superlattice confinement plays no part in governing the transition field, and hence a reduction in superlattice confinement will not result in a further increase in transition

field. A InAs(210 Å)/GaSb(120 Å) superlattice will undergo the transition at ~90 T, as will the InAs/GaSb heterojunction.

IV. CONCLUSIONS

We have used a microscopic complex-band-structure approach to study the magnetic field induced semimetal-to-semiconductor transition in InAs/GaSb superlattices. The magnetic field is applied parallel to the interfaces rather than in a more conventional perpendicular direction. This results in a much higher required magnetic field to cause the transition than in the perpendicular geometry since the effect of magnetic confinement is reduced. The transition is a function of superlattice period until the layer widths become wide enough for bulk states to appear in the center of the layers, after which there will be no increase in transition field with an increasing layer thickness. The maximum in-plane magnetic field required to cause the semimetal-to-semiconductor transition in InAs/GaSb heterostructures is found to be ~90 T, and occurs when the InAs and GaSb layer widths are greater than ~120 Å.

ACKNOWLEDGMENTS

A.R.R. has been supported by EPSRC(UK). We thank Dr. Z. Ikonić and Dr. W. Tan for useful discussions. The computational work has been supported by the EPSRC(UK) through the CSI scheme.

[1] G. A. Sai-Halasz, R. Tsu, and L. Esaki, Appl. Phys. Lett. **30**, 651 (1977).
[2] D. J. Barnes, R. J. Nicholas, N. J. Mason, P. J. Walker, R. J. Warburton, and N. Miura, Physica B **184**, 168 (1993).
[3] R. J. Nicholas, K. S. H. Dalton, M. Lakrimi, C. Lopez, R. W. Martin, N. J. Mason, G. M. Summers, G. M. Sundaram, D. M. Symons, P. J. Walker, R. J. Warburton, M. I. Erements, D. J. Barnes, N. Miura, L. Van Bockstal, R. Bogaerts, and F. Herlach, Physica B **184**, 268 (1993).
[4] D. J. Barnes, R. J. Nicholas, R. J. Warburton, N. J. Mason, P. J. Walker, and N. Miura, Solid State Commun. **37**, 1027 (1994).
[5] G. M. Sundaram, R. J. Warburton, R. J. Nicholas, G. M. Summers, N. J. Mason, and P. J. Walker, Semicond. Sci. Technol. **7**, 985 (1992).
[6] D. J. Barnes, R. J. Nicholas, R. J. Warburton, N. J. Mason, P. J. Walker, and N. Miura Phys. Rev. B **49**, 10 474 (1994).
[7] Ikai Lo, W. C. Mitchel, and J.-P. Cheng, Phys. Rev. B **48**, 9118 (1993).
[8] A. Fasolino and M. Altarelli, Surf. Sci. **142**, 322 (1984).
[9] N. J. Kawai, L. L. Chang, G. A. Sai-Halasz, C. A. Chang, and L. Esaki, Appl. Phys. Lett. **36**, 369 (1980).
[10] S. Brand and D. T. Hughes, Semicond. Sci. Technol. **2**, 607 (1987).
[11] S. Brand and D. T. Hughes, Semicond. Sci. Technol. **2**, 123 (1987).
[12] Y. C. Chang and J. N. Schulman, Phys. Rev. B **25**, 3975 (1982).
[13] D. Y. K. Ko and J. C. Inkson, Phys. Rev. B **38**, 9954 (1988); **38**, 12 416 (1988).
[14] W. C. Tan, J. C. Inkson, and G. P. Srivastava, in *Quantum Well Intersubband Transition Physics and Devices*, Vol. 270 of *NATO Advanced Study Institute Series E: Applied Sciences*, edited by H. C. Liu, B. F. Levine and J. Y. Andersson (Kluwer, Boston, 1993).
[15] M. L. Cohen and T. K. Bergstresser, Phys. Rev. **141**, 789 (1966).
[16] See, for example, C. Kittel, *Introduction to Solid State Physics* (Wiley, New York, 1986).
[17] The form factors $v(|\underline{G}|)$ (in Rydbergs) used are $v_A^3 = -0.2700e0(-0.2200e0)$; $v_A^8 = +0.0060e0(+0.0012e0)$; $v_A^{11} = +0.0590e0(+0.0484e0)$; $v_S^3 = +0.0630e0(+0.0820e0)$; $v_S^3 = +0.0630e0(+0.0820e0)$; $v_S^4 = +0.0500e0(+0.0500e0)$; $v_S^{11} = +0.0100e0$ (+0.0300e0) for GaSb (InAs).
[18] G. Weisz, Phys. Rev. **149**, 504 (1966).
[19] J. C. Inkson, W. Tan, and G. Edwards, Semicond. Cond. Sci. Technol. **9**, 113 (1993).
[20] G. A. Sai-Halasz, L. Esaki, and W. A. Harrison, Phys. Rev. B **18**, 2812 (1978).
[21] D. Y. K. Ko, G. Edwards, and J. C. Inkson, Semi. Cond. Sci. Tech. **5**(3), 200 (1990).
[22] G. Bastard, *Wave Mechanics Applied to Semiconductor Heterostructures* (Les Éditions de Physique, Les Ulis, 1988).
[23] K. J. Moore *et al.*, Phys. Rev. B **42**, 3024 (1990).
[24] *Physics of Group IV Elements and III-V Compounds*, edited by K. -H. Hellwege and O. Madelung, Landolt-Börnstein, New Series, Group III, Vol. 17, Pt. a (Springer-Verlag, Berlin, 1982) and references therein.
[25] A. R. Rundell, G. P. Srivastava, and J. C. Inkson (unpublished).